

A Data Analytics Perspective of the Clarke and Related Transforms in Power Grid Analysis

Teaching Old Power Systems New Tricks

Danilo P. Mandic, Sithan Kanna, Yili Xia, Ahmad Moniri, and Anthony G. Constantinides

Affordable and reliable electric power is fundamental to modern society and economy, with the Smart Grid becoming an increasingly important factor in power generation and distribution. In order to fully exploit its advantages, the analysis of modern Smart Grid requires close collaboration and convergence between power engineers and signal processing and machine learning experts. Current analysis techniques are typically derived from a Circuit Theory perspective; such an approach is adequate for only fully balanced systems operating at nominal conditions and non-obvious for data scientists – this is prohibitive for the analysis of dynamically unbalanced smart grids, where Data Analytics is not only well suited but also necessary. A common language that bridges the gap between Circuit Theory and Data Analytics, and the respective community of experts, would be a natural step forward. To this end, we revisit the Clarke and related transforms from a subspace, latent component, and spatial frequency analysis frameworks, to establish fundamental relationships between the standard three-phase transforms and modern Data Analytics. We show that the Clarke transform admits a physical interpretation as a “spatial dimensionality” reduction technique which is equivalent to Principal Component Analysis (PCA) for balanced systems, but is sub-optimal for dynamically unbalanced systems, such as the Smart Grid, while the related Park transform performs further “temporal” dimensionality reduction. Such a perspective opens numerous new avenues for the use Signal Processing and Machine Learning in power grid research, and paves the way for innovative optimisation, transformation, and analysis techniques that are not accessible to arrive at from the standard Circuit Theory principles, as demonstrated in this work through the possibility of simultaneous frequency estimation and fault detection via adaptive Clarke and Park transforms. In addition, the introduced seamless transition between the Circuit Theory concepts and Data Analytics ideas promises to provide a straightforward and unifying platform for further the understanding of sources of imbalance in modern power grids, together with an avenue for learning strategies, optimal parameter selection, and enhanced interpretation of Smart Grid problems and new avenues for the mitigation of these issues. In addition, the material may be useful in lecture courses in multidisciplinary research from Smart Grid to Big Data, or indeed, as interesting reading for the intellectually curious and generally knowledgeable reader.

Tribute to Edith Clarke, a pioneer of power grid analysis

Edith Clarke (1883-1959) is a true pioneer in the application of circuit theory and mathematical techniques to electrical power systems. She was the first woman to obtain an M.S. in Electrical Engineering from MIT, in 1919, and the first female professor of Electrical Engineering in the USA, having been appointed at the University of Texas at Austin, in 1947. Her pivotal contributions were concerned with the development of algorithms for the simplification of the laborious computations involved in the design and operation of electrical power systems [1]. One of her early inventions was the Clarke calculator (1921), a graphical device that solved power system equations 10 times faster than a human computer [2]. The Clarke transform, also known as the $\alpha\beta$ transform, was introduced by Edith Clarke in 1943, and has since been established as a fundamental and indispensable tool for the analysis of three-phase power systems. With the advent of Smart Grid, the Clarke transform represents an underpinning technology for signal processing, control and machine learning applications related state estimation, frequency tracking, and fault detection [3–5], the most important aspects in the development of the future Smart Grid.

Challenges in Smart Grid: A Fertile Ground for Data Analytics

There is substantial interest in transforming the way we both produce and use energy as current ways are not sustainable. For the electrical power grid this involves fundamental paradigm shifts as we build a smart grid, adopt more renewable energy sources, and promote more energy efficient practices. A smart grid delivers electricity from suppliers to users using digital technology and has a number of properties including incorporating all forms of energy generation and storage, using sensor information, enabling active participation by end users, being secure and reliable, and using optimization and control to make decisions; see for example, the Energy Independence and Security Act 2007, Section 1304 Smart Grid RD&D Highlights. This will require fundamental shifts in the way we analyse and design power systems and prominent involvement of modern Data Analytics disciplines which are currently outside the standard Power Systems, such as those enabled by Signal Processing and Machine Learning. Although we have just begun to investigate a whole host of e.g. Signal Processing issues for the smart grid strategy, these new technologies will undoubtedly be critical to the efficient use of limited and intermittent power resources in the future. The first and fundamental step in this direction is to bridge the gap between the Power Systems community and the Data Analytics communities by establishing a common language for the understanding and interpretation of system behaviour, the aim of this Perspective.

Economic Value of the Smarter Grid. To depict the sheer scale of the required changes to current practice, we summarise the recent findings from [6]:

- The Brattle Group has estimated that the investment needed to replace old generation of power plants with the new ones would be about USD 560 billion by 2030;
- In the USA, about 40% of human-caused emissions of CO_2 are due to generation of electricity;
- If the power grids were just 5% more efficient, the resultant energy and emission reductions would be equivalent to permanently eliminating 53 million cars;
- Capacity to meet demand during the top 100 peak hours in the year accounts for 10-20% of total electricity costs;
- The cost of outages to the USA economy is about USD 80 billion annually.

Yet, current centralised power plants are at best 35% efficient while the renewable sources affect the stability and inertia in current power systems and are therefore not used to their full capacity.

Power Quality Issues. System frequency is the most important power quality parameter; its rise indicates more generation than consumption while a decrease indicates less generation than consumption. The IEEE 1547 Standard specifies that a distributed generation source must disconnect from a locally islanded system within 2 seconds; it also requires disconnecting for sagging voltage under high demand (voltage sags are described by the IEEE Standard 1159–1995). However, disconnecting a large number of local generators (e.g. solar) can cause the low-voltage condition to accelerate [6], and can also affect the current way of estimating power quality parameters (frequency, voltage phasors). This all calls for accurate frequency estimator which are robust under unbalanced system conditions.

Current estimation in three-phase systems is routinely performed through the Clarke and related transforms, which are designed for stable grids operating in nominal conditions. However, smart grids introduce dynamically unbalanced conditions which yield incorrect frequency estimates due to [7–9]:

- Inadequacy of the Clarke and related transforms for unbalanced system conditions;
- False frequency estimates when the system is experiencing voltage sags, that is, off-nominal amplitudes and/or phases of the three phase voltages, even if the systems frequency remains at a nominal $\omega_o \in \{50Hz, 60Hz\}$;
- Some loads (furnaces, cyclo-converters) introduce inter-harmonics that are not integer multiples of the fundamental frequency. These cannot be estimated using spectral techniques and tend to drift over time thus affecting systems prone to resonance (low damping or a high Q factor).

Opportunities for Data Analytics Research. Three-phase systems can be inherently difficult to analyse as the electrical quantities involved are coupled by design while also exhibiting redundancies.

During her early career as a human “computer” with the General Electric company, Edith Clarke routinely faced problems related to the simplification of the analyses of three-phase circuits. Fast forward a century, and three-phase systems pose another class of practical problems, essentially of a signal processing and machine learning nature which include:

- In smart grids, the effects arising from the on–off switching of various subgrids and the dual roles of generators/loads will produce transients and spurious frequency/phasor estimates; the analysis thus requires modern Signal Processing and Machine Learning techniques;
- Accurate change of frequency trackers and rapid frequency estimators are a pre–requisite for the operation of smart grid, but their design is beyond the remit of Power Systems engineering;
- Rapid frequency trackers are envisaged to be part of many appliances, as in Smart Grid we not only must dynamically bring in new generators and interconnect the grid, but also smart loads must be able to detect rapid frequency changes and take action;
- Loss of mains detection from voltage dips and off–nominal frequencies is critical for system balance, these imbalances will be much more prominent in low–inertia grids of the future;
- Current analyses compute features over a predefined time interval, such as 200ms, 3s, 1m, 10m, 2h. These are adequate for standard grids with power reserve and high inertia (International Standard IEC 6100-4-30). For example, the PQ variations are currently calculated over a 200ms window – too coarse for rapid and real–time monitoring and analysis in smart grids where the required time scales are in the region of 2ms and below.

All in all, it is critical that frequency/phasor estimator remain accurate during the various interconnections, transients, faults, and voltage sags (IEEE Standard 1159–1995), while at the same time having intelligence to indicate whether the system experienced 1–, 2– or 3–phase fault; this “smart frequency” area has been subject of some recent patents [10] and ongoing research [5, 11–16].

Sources of Redundancy in Power System Analysis

We shall start by investigating the redundancy of information–bearing signals in three-phase systems, in order to establish a link between the current Circuit Theory inspired dimensionality reduction techniques and a more general Latent Component Analysis (LCA) view rooted in Data Analytics.

Exploiting Redundancy in Three-Phase Signal Representation

Consider a sampled three-phase voltage measurement vector, \mathbf{s}_k , which at a discrete time instant k , is given by

$$\mathbf{s}_k = \begin{bmatrix} v_{a,k} \\ v_{b,k} \\ v_{c,k} \end{bmatrix} = \begin{bmatrix} V_a \cos(\omega k + \phi_a) \\ V_b \cos(\omega k + \phi_b - \frac{2\pi}{3}) \\ V_c \cos(\omega k + \phi_c + \frac{2\pi}{3}) \end{bmatrix}, \quad (1)$$

where V_a, V_b, V_c are the amplitudes of the phase voltages $v_{a,k}, v_{b,k}, v_{c,k}$, while $\omega = 2\pi fT$ is the fundamental angular frequency, with f the fundamental power system frequency and T the sampling interval. The phase values for phase voltages are denoted by ϕ_a, ϕ_b , and ϕ_c .

Remark 1. *The three-phase power system is considered to be in a balanced condition if*

1. *The magnitudes of the phase voltages in (1) are equal, that is, $V_a = V_b = V_c$,*
2. *The phase angle separation between the phase voltages is uniform and equal to $\frac{2\pi}{3}$, that is, $\phi_a = \phi_b = \phi_c$, across the phase voltages.*

Early power engineers were able to effectively reduce the dimensionality in representing the three-phase signal in (1) **by changing the reference frame (or basis) of the three–phase power voltage signal**, the so–called voltage transformations [17]. Figure 1 illustrates effects of the three-phase transformations considered in this paper – the Clarke Transform and the closely related Park Transform.

Remark 2. Figure 1 allows us to provide a modern interpretation of the operation of the Clarke and Park transforms, whereby the Clarke Transform reduces the three-dimensional “spatial information space” in three-phase power signals to the two-dimensional $\alpha\beta$ space, while the Park transform applies a two-dimensional time-varying basis to the Clarke transform, in the form of a rotation matrix whose bases rotate at the fundamental power system frequency of 50 Hz, to further reduce the “temporal information space” to only two constants, v_d and v_q .

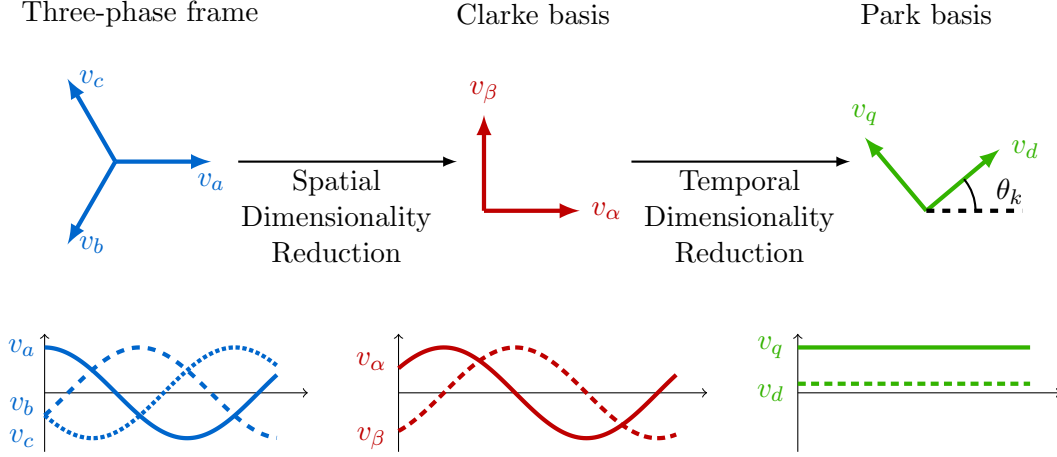


Figure 1: Geometric interpretation of the Clarke and Park Transforms through the corresponding “spatial” and “temporal” dimensionality reductions.

Signal Processing View of Spatial Redundancy in Three-Phase Power Systems

We now show that the three-phase power signal in (1) is essentially over-parametrised, thus paving the way for a Data Analytics perspective of the Clarke Transform. To this end, consider the empirical covariance matrix of the three-phase voltage signal, \mathbf{s}_k in (1), defined as $\text{cov}(\mathbf{s}_k) \stackrel{\text{def}}{=} \mathbf{R}_s$, which can be computed from N consecutive samples of \mathbf{s}_k as

$$\mathbf{R}_s = \lim_{N \rightarrow \infty} \frac{1}{N} \sum_{k=0}^{N-1} \mathbf{s}_k \mathbf{s}_k^H, \quad (2)$$

where the symbol $(\cdot)^H$ denotes the Hermitian transpose operator.

Phasor representation. From the three-phase voltage, \mathbf{s}_k in (1), upon employing the identity $\cos(x) = (e^{jx} + e^{-jx})/2$, we arrive at its phasor representation in the form

$$\mathbf{s}_k = \frac{1}{2} \begin{bmatrix} \bar{V}_a \\ \bar{V}_b \\ \bar{V}_c \end{bmatrix} e^{j\omega k} + \frac{1}{2} \begin{bmatrix} \bar{V}_a^* \\ \bar{V}_b^* \\ \bar{V}_c^* \end{bmatrix} e^{-j\omega k} \quad (3)$$

where, for compactness, the time-independent phasors, $\bar{V}_a = \frac{V_a}{\sqrt{2}} e^{j\phi_a}$, $\bar{V}_b = \frac{V_b}{\sqrt{2}} e^{j(\phi_b - \frac{2\pi}{3})}$ and $\bar{V}_c = \frac{V_c}{\sqrt{2}} e^{j(\phi_c + \frac{2\pi}{3})}$, can be comprised into the phasor vector

$$\mathbf{v} \stackrel{\text{def}}{=} [\bar{V}_a, \bar{V}_b, \bar{V}_c]^T. \quad (4)$$

Without loss of generality, we shall consider normalised versions of the phasors (relative to \bar{V}_a), and define $\delta_i \stackrel{\text{def}}{=} \bar{V}_i / \bar{V}_a$, $i \in \{a, b, c\}$, with $\delta_a = 1$, to give

$$\mathbf{s}_k = \frac{1}{2} \left(\mathbf{v} e^{j\omega k} + \mathbf{v}^* e^{-j\omega k} \right) \quad (5)$$

so that the normalised version of the phasor vector, \mathbf{v} in (4), now becomes

$$\mathbf{v} = [1, \delta_b, \delta_c]^\top. \quad (6)$$

In order to arrive at the final expression for the empirical covariance matrix, \mathbf{R}_s in (2), observe from (5) that the individual outer products, $\mathbf{s}_k \mathbf{s}_k^\mathbf{H}$ in (2), represent an average of four outer products, that is

$$\mathbf{s}_k \mathbf{s}_k^\mathbf{H} = \frac{1}{4} \left(\mathbf{v} \mathbf{v}^\mathbf{H} + \mathbf{v}^* \mathbf{v}^\mathbf{T} + \mathbf{v} \mathbf{v}^\mathbf{T} e^{2j\omega k} + \mathbf{v}^* \mathbf{v}^\mathbf{H} e^{-2j\omega k} \right). \quad (7)$$

For $\omega \neq 0$ or $\omega \neq \pi$, and for a large enough N , the following holds [18, p. 56]

$$\lim_{N \rightarrow \infty} \frac{1}{N} \sum_{k=0}^N e^{\pm 2j\omega k} = 0, \quad (8)$$

so that the last two outer products in (7) vanish and the individual outer product within the covariance matrix for a general 3-phase power voltage measurement become

$$\mathbf{s}_k \mathbf{s}_k^\mathbf{H} = \frac{1}{4} \left(\mathbf{v} \mathbf{v}^\mathbf{H} + \mathbf{v}^* \mathbf{v}^\mathbf{T} \right) = \frac{1}{2} \operatorname{Re} \left\{ \mathbf{v} \mathbf{v}^\mathbf{H} \right\} = \frac{1}{2} \left(\mathbf{v}_r \mathbf{v}_r^\mathbf{T} + \mathbf{v}_i \mathbf{v}_i^\mathbf{T} \right), \quad (9)$$

where $\mathbf{v}_r = \operatorname{Re} \{ \mathbf{v} \}$ and $\mathbf{v}_i = \operatorname{Im} \{ \mathbf{v} \}$ denote the real and imaginary part of the phasor vector \mathbf{v} defined in (6).

Remark 3. Observe from (9) that the 3×3 covariance matrix, \mathbf{R}_s in (2), of the trivariate three-phase voltage signal, \mathbf{s}_k , is rank-deficient (Rank-2) as it represents a sum of two Rank-1 outer products, $\mathbf{v}_r \mathbf{v}_r^\mathbf{T}$ and $\mathbf{v}_i \mathbf{v}_i^\mathbf{T}$. In other words, without loss in information the three-phase signal in (3) can be projected onto a two-dimensional subspace spanned by $\mathbf{v}_r \mathbf{v}_r^\mathbf{T}$ and $\mathbf{v}_i \mathbf{v}_i^\mathbf{T}$. This implies that the use of all three data channels (system phases) is redundant in the analysis, and offers a Data Analytics justification for the Clarke Transform.

We next proceed with the formal definition of the Clarke Transform, and show that its dimensionality reduction principle admits a Principal Component Analysis (PCA) interpretation.

Clarke Transform – A Fundamental Tool in Power System Analysis

The Clarke transform, also known as the $\alpha\beta$ transform, was introduced from a Circuit Theory viewpoint and aims to change the basis of the original vector space where the three-phase signal \mathbf{s}_k in (1) resides, to a basis defined by the columns of the so-called Clarke matrix, to yield the Clarke-transformed $v_{0,k}, v_{\alpha,k}, v_{\beta,k}$ voltages in the form

$$\begin{bmatrix} v_{0,k} \\ v_{\alpha,k} \\ v_{\beta,k} \end{bmatrix} = \underbrace{\sqrt{\frac{2}{3}} \begin{bmatrix} \frac{\sqrt{2}}{2} & \frac{\sqrt{2}}{2} & \frac{\sqrt{2}}{2} \\ 1 & -\frac{1}{2} & -\frac{1}{2} \\ 0 & \frac{\sqrt{3}}{2} & -\frac{\sqrt{3}}{2} \end{bmatrix}}_{\text{Clarke matrix}} \underbrace{\begin{bmatrix} v_{a,k} \\ v_{b,k} \\ v_{c,k} \end{bmatrix}}_{\mathbf{s}_k}, \quad (10)$$

The quantities $v_{\alpha,k}$ and $v_{\beta,k}$ are referred to as the α and β sequences, while the term $v_{0,k}$ is called the zero-sequence, as it is null when the three-phase signal \mathbf{s}_k is balanced (see Remark 1).

Remark 4. The traditional power grid is typically in a balanced condition due to its huge inertia, and therefore, only $v_{\alpha,k}$ and $v_{\beta,k}$ are used in its analysis since balanced phase voltages yield $v_{0,k} = 0$. The “standard” version of the Clarke transform thus employs only the last two rows of the Clarke matrix in (10), to project the three-phase voltage in (1) onto a 2D subspace spanned by these columns, that is

$$\begin{bmatrix} v_{\alpha,k} \\ v_{\beta,k} \end{bmatrix} = \underbrace{\sqrt{\frac{2}{3}} \begin{bmatrix} 1 & -\frac{1}{2} & -\frac{1}{2} \\ 0 & \frac{\sqrt{3}}{2} & -\frac{\sqrt{3}}{2} \end{bmatrix}}_{\text{Reduced Clarke matrix: } \mathbf{C}} \begin{bmatrix} v_{a,k} \\ v_{b,k} \\ v_{c,k} \end{bmatrix}. \quad (11)$$

This is further visualised in Figure 2 which provides a geometric interpretation of the Clarke transform for balanced power systems. Observe the mutually orthogonal nature of the $v_{\alpha,k}$ and $v_{\beta,k}$ components, which allows for their convenient combination into a complex-valued voltage, $s_k = v_{\alpha,k} + jv_{\beta,k}$.

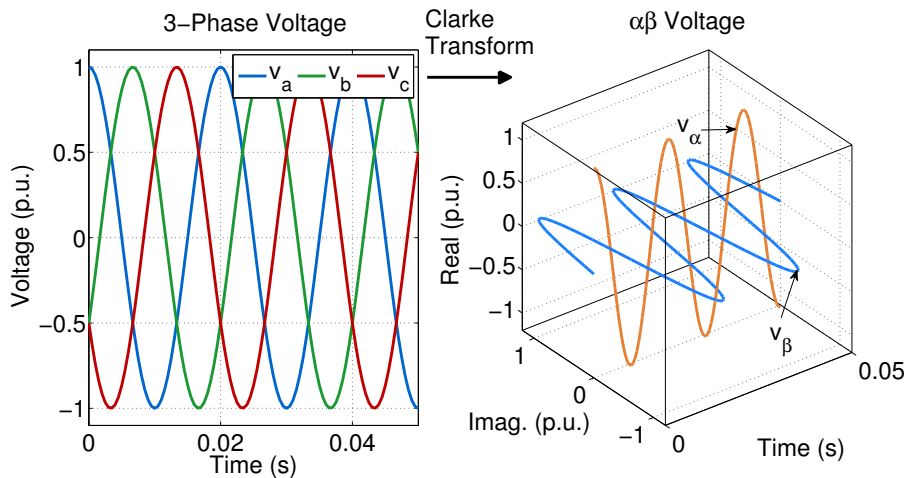


Figure 2: Waveforms of Clarke-transformed three-phase voltages. The Clarke voltages v_α and v_β are orthogonal and admit a convenient complex valued representation in the form $s_{i,k} = v_{\alpha,i,k} + jv_{\beta,i,k}$.

Park Transform

The Park transform (also known as the dq transform) is closely related to Clarke Transform and projects the three-phase signal \mathbf{s}_k onto an orthogonal, time-varying frame which, by virtue of rotating at the fundamental power system frequency ω_\circ (50 Hz or 60 Hz), yields stationary constant outputs, $v_{d,k}, v_{q,k}$. In other words, the Park voltages $v_{d,k}, v_{q,k}$ are obtained from the Clarke's $\alpha\beta$ voltages in (11) using a time-varying transformation given by [19]

$$\begin{bmatrix} v_{d,k} \\ v_{q,k} \end{bmatrix} = \underbrace{\begin{bmatrix} \cos(\theta_k) & \sin(\theta_k) \\ -\sin(\theta_k) & \cos(\theta_k) \end{bmatrix}}_{\text{Park Matrix: } \mathbf{P}_\theta} \begin{bmatrix} v_{\alpha,k} \\ v_{\beta,k} \end{bmatrix}. \quad (12)$$

where $\theta_k = \omega_\circ k$, while the orthogonal direct and quadrature components, $v_{d,k}$ and $v_{q,k}$, can be combined into a complex variable $v_k = v_{d,k} + jv_{q,k}$.

Remark 5. From the modern Data Analytics perspective, the Park matrix, \mathbf{P}_θ , is a full-rank and time-varying clock-wise rotation matrix, with the determinant $\det(\mathbf{P}_\theta) = 1$ and the unit-norm eigenvalues $|\lambda_{1,2}| = 1$. It therefore does not amplify the original Clarke vector $[v_{\alpha,k}, v_{\beta,k}]^T$ but only rotates it, with the speed of rotation equal to the fundamental frequency of the power system, ω_\circ .

Figure 3 offers a geometric interpretation of the Clarke and Park transform of the three-phase voltage vector \mathbf{s}_k . Observe that, while the Clarke transform matrix, \mathbf{C} in (11) projects a 3D vector, \mathbf{s}_k , onto a two-dimensional space spanned by its columns, the Park transform matrix, \mathbf{P}_θ in (12), is a time-varying two-dimensional rotation matrix which changes only the direction of the 2-dimensional Clarke vector $[v_{\alpha,k}, v_{\beta,k}]^T = \mathbf{C}\mathbf{s}_k$.

Principal Component Analysis (PCA)

Modern Data Analytics often employs Principal Component Analysis, in order to either separate meaningful data from noise, or to reduce the dimensionality of the original signal space while maintaining the most important information-bearing latent components in data. Consider a general data

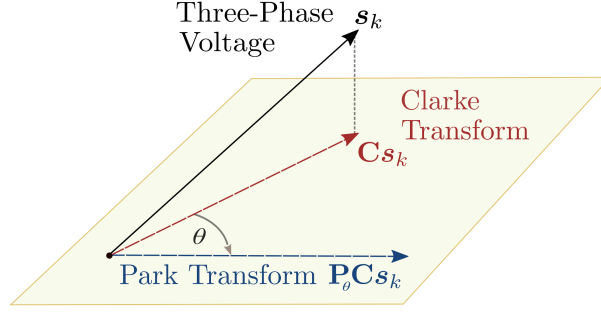


Figure 3: Geometric representation of the Clarke and Park three-phase transforms, applied to a three-phase voltage vector, \mathbf{s}_k .

vector, $\mathbf{x}_k \in \mathbb{R}^{M \times 1}$, for which the covariance matrix is defined as

$$\text{cov}(\mathbf{x}_k) \stackrel{\text{def}}{=} \mathbf{R}_x = \lim_{N \rightarrow \infty} \frac{1}{N} \sum_{k=0}^{N-1} \mathbf{x}_k \mathbf{x}_k^\top. \quad (13)$$

Then, this symmetric covariance matrix \mathbf{R}_x admits the following eigenvalue decomposition

$$\mathbf{Q}^\top \mathbf{R}_x \mathbf{Q} = \mathbf{\Lambda} \quad (14)$$

where the diagonal eigenvalue matrix, $\mathbf{\Lambda} = \text{diag}\{\lambda_1, \lambda_2, \dots, \lambda_M\}$, indicates the power of each component within \mathbf{x}_k , while the matrix of eigenvectors, $\mathbf{Q}_r = [\mathbf{q}_1, \mathbf{q}_2, \dots, \mathbf{q}_M]$, designates the principal directions in the data.

Suppose the signal \mathbf{x}_k is to be transformed into a vector, $\mathbf{u}_k \in \mathbb{R}^{M \times 1}$, with the same dimensionality as the original signal \mathbf{x}_k , using a linear transformation matrix \mathbf{W} , to give

$$\mathbf{u}_k = \mathbf{W} \mathbf{x}_k, \quad \text{where} \quad \text{cov}(\mathbf{u}_k) = \mathbf{\Lambda}. \quad (15)$$

The principal component analysis (PCA), also known as the Karhunen-Loeve transform, states that the above transformation matrix, \mathbf{W} , can be obtained from the eigenvector and eigenvalue matrices in (14) as $\mathbf{W} = \mathbf{Q}^\top$ [20]. In other words,

$$\begin{aligned} \text{cov}(\mathbf{u}_k) &= \lim_{N \rightarrow \infty} \frac{1}{N} \sum_{k=0}^{N-1} \mathbf{u}_k \mathbf{u}_k^\top \\ &= \mathbf{W} \left(\lim_{N \rightarrow \infty} \frac{1}{N} \sum_{k=0}^{N-1} \mathbf{x}_k \mathbf{x}_k^\top \right) \mathbf{W}^\top \\ &= \mathbf{Q}^\top \mathbf{R}_x \mathbf{Q} = \mathbf{\Lambda} \end{aligned} \quad (16)$$

This formulation admits a convenient dimensionality reduction by retaining only $r < M$ largest eigenvalues and the corresponding eigenvectors of \mathbf{R}_x . The so obtained transformed data vector, $\mathbf{u}_{r,k} \in \mathbb{R}^{r \times 1}$, is of dimension $r < M$ and is given by

$$\mathbf{u}_{r,k} = \mathbf{Q}_{1:r}^\top \mathbf{x}_k \quad (17)$$

where $\mathbf{Q}_{1:r} = [\mathbf{q}_1, \mathbf{q}_2, \dots, \mathbf{q}_r]$, while r stands for the r largest eigenvalues in $\mathbf{\Lambda}$. In other words, the PCA-based dimensionality reduction scheme in (17) selects the directions in which the data expresses maximum variance, designated by the directions of the principal eigenvectors of the data covariance matrix, \mathbf{R}_x .

Clarke Transform as a Principal Component Analyser

We have seen that for a balanced power system, the phasor vector, \mathbf{v} in (6), takes the form

$$\mathbf{v} = \left[1, e^{-j\frac{2\pi}{3}}, e^{j\frac{2\pi}{3}} \right]^T \quad (18)$$

so that the covariance matrix of the normalised three-phase power signal, \mathbf{s}_k , now becomes

$$\mathbf{R}_s = \frac{1}{2} \text{Re} \{ \mathbf{v} \mathbf{v}^H \} = \frac{1}{4} \begin{bmatrix} 2 & -1 & -1 \\ -1 & 2 & -1 \\ -1 & -1 & 2 \end{bmatrix}. \quad (19)$$

and thus admits the eigen-decomposition in (14), to yield

$$\mathbf{R}_s = \mathbf{Q} \mathbf{\Lambda} \mathbf{Q}^T. \quad (20)$$

By inspection of \mathbf{R}_s in (19), from the first eigenvector-eigenvalue pair, $(\mathbf{q}_1, \lambda_1)$, we have

$$\mathbf{R}_s \mathbf{q}_1 = \mathbf{0} \implies \mathbf{q}_1 = \frac{1}{\sqrt{3}} \mathbf{1}, \lambda_1 = 0. \quad (21)$$

To find the remaining eigenvector-eigenvalue pairs, consider again the outer products within the covariance matrix, given in (9), and the normalised phasor vector, \mathbf{v} in (18). Notice that its real part, $\mathbf{v}_r = \text{Re} \{ \mathbf{v} \} = [1, -\frac{1}{2}, -\frac{1}{2}]^T$, and its imaginary part, $\mathbf{v}_i = \text{Im} \{ \mathbf{v} \} = [0, -\frac{\sqrt{3}}{2}, \frac{\sqrt{3}}{2}]^T$, are orthogonal, that is, $\mathbf{v}_r^T \mathbf{v}_i = 0$.

Therefore, the remaining two eigenvectors of \mathbf{R}_s are $\mathbf{q}_2 = \mathbf{v}_r / \|\mathbf{v}_r\|$ and $\mathbf{q}_3 = \mathbf{v}_i / \|\mathbf{v}_i\|$ with the corresponding eigenvalues, $\lambda_2 = \frac{1}{4} \|\mathbf{v}_r\|^2$ and $\lambda_3 = \frac{1}{4} \|\mathbf{v}_i\|^2$, so that the matrix of eigenvectors, \mathbf{Q}^T , and the diagonal matrix of eigenvalues, $\mathbf{\Lambda}$, in (20) take the form

$$\mathbf{Q}^T = \sqrt{\frac{2}{3}} \begin{bmatrix} \frac{\sqrt{2}}{2} & \frac{\sqrt{2}}{2} & \frac{\sqrt{2}}{2} \\ 1 & -\frac{1}{2} & -\frac{1}{2} \\ 0 & \frac{\sqrt{3}}{2} & -\frac{\sqrt{3}}{2} \end{bmatrix} \quad \mathbf{\Lambda} = \frac{1}{4} \begin{bmatrix} 0 & 0 & 0 \\ 0 & 1.5 & 0 \\ 0 & 0 & 1.5 \end{bmatrix}. \quad (22)$$

Inspection of the diagonal elements of $\mathbf{\Lambda}$ in (22) reveals only two non-zero eigenvalues. This verifies Remark 3 which states that the covariance matrix of a three-phase power system voltage, \mathbf{R}_s , is of Rank-2 and thus rank-deficient. The factor $\sqrt{2/3}$ which pre-multiplies \mathbf{Q}^T in (22) serves to normalise the length of the eigenvectors to unity (ortho-normality).

Remark 6. *The matrix of eigenvectors, \mathbf{Q}^T in (22), is identical to the Clarke transformation matrix defined in (10). Therefore, all of the variance in three-phase power system voltages can be explained by the two eigenvectors associated with the non-zero eigenvalues (principal axes) of the Clarke-transform-matrix. This offers the modern, Data Analytics, interpretation of Clarke's transform as a Principal Component Analyser which performs a projection of three-phase power systems in \mathbb{R}^3 onto a 2D subspace spanned by the two largest orthogonal eigenvectors of the phase-voltage correlation matrix, $[1, -\frac{1}{2}, -\frac{1}{2}]^T$ and $[0, \frac{\sqrt{3}}{2}, -\frac{\sqrt{3}}{2}]^T$, as illustrated in Figure 4.*

Remark 7. *Remark 6 and Figure 4 offer a modern interpretation of the Clarke transform from a PCA-based dimensionality reduction viewpoint. Such new perspective opens numerous new avenues for the use of Data Analytics (such as Signal Processing and Machine Learning) in power grid research, and paves the way for innovative transformation and analysis techniques for the future Smart Grid – not possible to achieve from the standard Circuit Theory principles.*

We shall next illuminate the power of Data Analytics in Smart Grid design and analysis, by exploring new self-stabilising Clarke-inspired transforms, which unlike the original method adapt automatically to the dynamically unstable Smart Grid conditions.

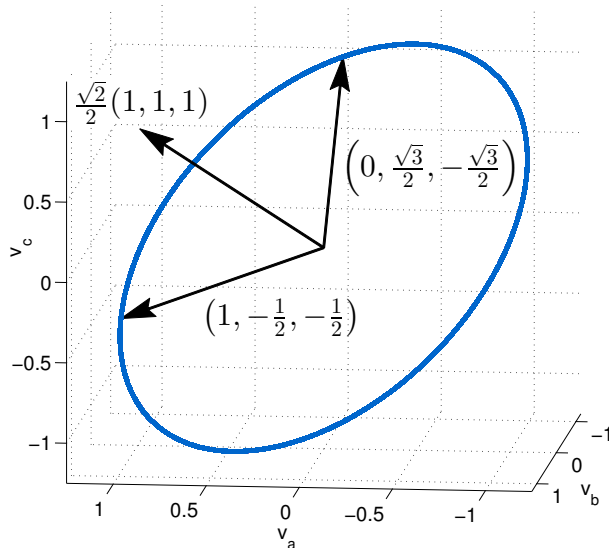


Figure 4: A balanced three-phase power system with three principal axes. Notice that all information is contained within a 2D subspace spanned by the eigenvectors $[1, -\frac{1}{2}, -\frac{1}{2}]$ and $[0, \frac{\sqrt{3}}{2}, -\frac{\sqrt{3}}{2}]$, that is, in a space defined by the PCA which retains the two largest eigenvalues/eigenvectors of the corresponding covariance matrix, \mathbf{R}_s . In other words, balanced three-phase power systems exhibit only two degrees of freedom.

Meeting the Needs of Smart Grid: A Dynamic Clarke Transform for Unbalanced Power Systems

It is a pre-requisite for future smart grids to move away from the traditional high-inertia load-following operating strategy to a dynamic scenario which involves low inertia, smart loads and renewable generation, which causes the three-phase systems to operate in a dynamically unbalanced condition. This, in turn, yields unequal phase voltages and non-uniform phase separations which need to be catered for in real time.

Clarke and Symmetric transforms as a 3-point DFT

We shall now offer an interpretation of the the well-known inadequacy of current power system analysis techniques in unbalanced grid scenarios, through a link with the effects of incoherent sampling in spectral analysis.

Symmetrical Transform as a Spatial Discrete Fourier Transform (DFT). The vector of three-phase time-domain voltages, \mathbf{s}_k in (1), is typically considered as a collection of three univariate signals. However, observe that the phase voltage samples within \mathbf{s}_k can also be treated as three samples of a monocomponent signal rotating at a *spatial frequency* $\Omega = -\frac{2\pi}{3}$. From this viewpoint, the phasor vector, \mathbf{v} in (4), in a balanced system is given by

$$\mathbf{v} = [1, e^{j\Omega}, e^{j2\Omega}]^T. \quad (23)$$

It is now obvious that \mathbf{v} can be treated as a single sinusoid rotating at a spatial frequency of $\Omega = -\frac{2\pi}{3}$, whereby the elements of \mathbf{v} are the corresponding phase voltages $v_{a,k}$, $v_{b,k}$, and $v_{c,k}$.

Remark 8. *Under unbalanced conditions, the phasor vector, \mathbf{v} , does not represent a single complex-valued spatial sinusoid since it contains the individual phasors with different amplitudes and a non-uniform phase separation, as defined in (4).*

Consider now the DFT of the phasor vector, $\mathbf{v} = [v_0, v_1, v_2]^T \in \mathbb{C}^{3 \times 1}$, given by

$$X[k] = \frac{1}{\sqrt{3}} \sum_{n=0}^2 v_n e^{-j \frac{2\pi}{3} nk}, \quad k = 0, 1, 2$$

which can be expressed in an equivalent matrix form

$$\begin{bmatrix} X[0] \\ X[1] \\ X[2] \end{bmatrix} = \frac{1}{\sqrt{3}} \begin{bmatrix} 1 & 1 & 1 \\ 1 & a & a^2 \\ 1 & a^2 & a \end{bmatrix} \begin{bmatrix} \bar{V}_a \\ \bar{V}_b \\ \bar{V}_c \end{bmatrix} \quad (24)$$

where $a = e^{-j \frac{2\pi}{3}}$. The three-point DFT in (24) therefore transforms the phasor vector \mathbf{v} into a stationary component $X[0]$ and two other components, $X[1]$ and $X[2]$, which rotate at the respective spatial frequencies $\frac{2\pi}{3}$ and $-\frac{2\pi}{3}$.

Remark 9. *The spatial DFT in (24) is identical to the Symmetrical Component Transform in (25). More specifically, the stationary DFT component, $X[0]$, corresponds to the zero-sequence phasor, \bar{V}_0 , while the fundamental DFT components, $X[1]$ and $X[2]$, represent respectively the positive- and negative-sequence phasors. This forms a basis for the treatment of three-phase component transforms from a Spectral Estimation perspective, and offers enhanced interpretation of the imperfections of these transforms in Smart Grid problems together with new avenues for the mitigation of these issues.*

Signal Processing interpretation. Observe that the spatial sampling in (23) represents a crude critical sampling where the system frequency is contained in the first component of the underlying 3-point DFT, with no provision for the interpretation of drifting frequencies, as required by the Smart Grid. This explains the well known inability of the Symmetrical Component Transform to deal with transients in three-phase power systems, and the relation with incoherent sampling artefacts – a standard issue in crudely sampled systems.

Dealing with unbalanced phasors: The Symmetrical Transform

The Symmetrical Transform was introduced by Charles Fortesque in 1918 to enable the decomposition of general unbalanced three-phase systems into three separate balanced networks [21]. Unlike the Clarke and Park transforms, the symmetrical transform operates on the phasors (Fourier transforms) of the three-phase voltage, \mathbf{s}_k , and is given by

$$\begin{bmatrix} \bar{V}_0 \\ \bar{V}_+ \\ \bar{V}_- \end{bmatrix} = \frac{1}{\sqrt{3}} \underbrace{\begin{bmatrix} 1 & 1 & 1 \\ 1 & a & a^2 \\ 1 & a^2 & a \end{bmatrix}}_{\text{DFT matrix}} \begin{bmatrix} \bar{V}_a \\ \bar{V}_b \\ \bar{V}_c \end{bmatrix}, \quad (25)$$

where $a = e^{-j \frac{2\pi}{3}}$. The aim is to convert a general unbalanced phasor vector, $\mathbf{v} = [\bar{V}_a, \bar{V}_b, \bar{V}_c]^T$ in (4), into three separate balanced components, referred to as the zero-, positive- and negative-sequence phasors, denoted respectively by \bar{V}_0 , \bar{V}_+ , and \bar{V}_- . Although the Symmetrical Component Transform can be used to analyse both balanced and unbalanced systems, it only applies to voltages in the phasor domain.

Observe that the Clarke transform can be interpreted as the real part of the 3-point DFT matrix in (25), since the diagonalisation of the eigenvector matrix for circulant matrices yields the DFT matrix.

Real-time Smart Grid tasks require analytical tools suitable for time-domain signals, thereby motivating the need for online dimensionality reduction techniques.

A Data Analytics Interpretation

We shall define the the imbalance ratios in unbalanced power systems as, $\delta_b = |\delta_b|e^{j\angle\delta_b}$ and $\delta_c = |\delta_c|e^{j\angle\delta_c}$. These ratios depend on the type of imbalance and yield a three-phase voltage covariance matrix

$$\mathbf{R}_g^u = \frac{1}{2} \begin{bmatrix} 1 & |\delta_b| \cos(\angle\delta_b) & |\delta_c| \cos(\angle\delta_c) \\ |\delta_b| \cos(\angle\delta_b) & |\delta_b|^2 & |\delta_b||\delta_c| \cos(\angle\delta_b - \angle\delta_c) \\ |\delta_c| \cos(\angle\delta_c) & |\delta_b||\delta_c| \cos(\angle\delta_b - \angle\delta_c) & |\delta_c|^2 \end{bmatrix} \quad (26)$$

which is different from that for the balanced case in (2) and (9).

Remark 10. Notice that for unbalanced power systems, due to the system imperfections modelled by the imbalance ratios $\delta_b = |\delta_b|e^{j\angle\delta_b}$ and $\delta_c = |\delta_c|e^{j\angle\delta_c}$, the eigenvector and eigenvalue matrices of the phase-voltage covariance matrix in (26) are different from those for the balanced system in (2). This, in turn, implies that the projections within the Clarke matrix are no longer a perfect match for the three-phase voltages and also differ from the true Principal Components in data derived through PCA.

Figure 5 illustrates that, regardless of the imbalance level in the power system, the three-phase voltages still reside in a 2-dimensional subspace of \mathbb{R}^3 . However, as the type and level of system unbalance dynamically change, the “static” Clarke transform in (11) will no longer be identical to the optimal “correct” PCA based dimensionality reduction scheme derived in (22). This explains the well-known phenomenon that the application of the Clarke transform to unbalanced system voltages will spurious forms of $\alpha\beta$ voltages [5, 10].

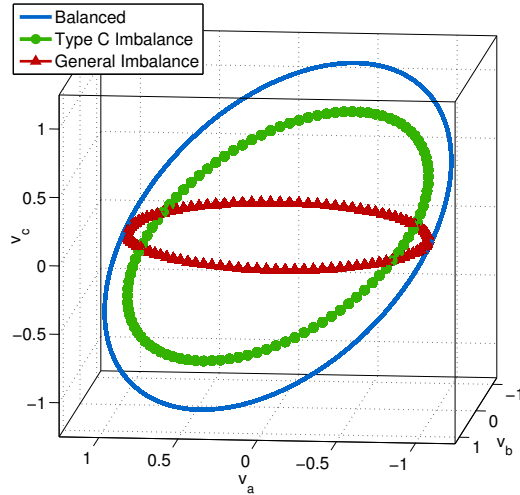


Figure 5: Scatter plot trajectories of the three-phase system voltages under: i) Balanced conditions (circle in blue); ii) Symmetric unbalanced condition for nominal frequency but unbalanced voltages (Type C voltage sag, ellipse in green); iii) General asymmetric imbalance for both off-nominal frequency and voltage imbalance (ellipse in red). Observe that independently of the type of imbalance, the Clarke voltages, v_α and v_β , will still reside in a 2D subspace of the 3D voltage space, but will no longer represent a perfect physically meaningful PCA-based dimensionality reduction scheme.

Power System Imbalance through the Lens of Complex Noncircular Statistics

To further depict problems associated with unbalanced power systems, we shall revisit the complex-domain representations of the Clarke and Park Transforms.

The Clarke’s $\alpha\beta$ voltage in (11) can be conveniently represented as a complex variable

$$s_k \stackrel{\text{def}}{=} v_{\alpha,k} + jv_{\beta,k}. \quad (27)$$

or directly from the Clarke matrix

$$s_k = \mathbf{c}^H \mathbf{s}_k, \quad \mathbf{c} \stackrel{\text{def}}{=} \sqrt{\frac{2}{3}} \left[1, e^{-j\frac{2\pi}{3}}, e^{j\frac{2\pi}{3}} \right]^T \quad (28)$$

where \mathbf{c} designates the complex Clarke transformation vector (see also (23)).

Upon combining with the original phasors from (3), the complex $\alpha\beta$ voltage, s_k , assumes a physically meaningful representation through the positive–sequence voltage, \bar{V}_+ , and the negative–sequence voltage, \bar{V}_- , in the form

$$s_k = \frac{1}{\sqrt{2}} \left(\bar{V}_+ e^{j\omega k} + \bar{V}_-^* e^{-j\omega k} \right), \quad (29)$$

where [22]

$$\begin{aligned} \bar{V}_+ &= \frac{1}{\sqrt{3}} \left[V_a e^{j\phi_a} + V_b e^{j\phi_b} + V_c e^{j\phi_c} \right] \\ \bar{V}_-^* &= \frac{1}{\sqrt{3}} \left[V_a e^{-j\phi_a} + V_b e^{-j\left(\phi_b + \frac{2\pi}{3}\right)} + V_c e^{-j\left(\phi_c - \frac{2\pi}{3}\right)} \right]. \end{aligned} \quad (30)$$

Remark 11. Notice that for balanced three–phase power systems, characterised by equal voltage magnitudes ($V_a = V_b = V_c$) and equal phase separations ($\phi_a = \phi_b = \phi_c$), the negative sequence voltage vanishes, that is, $\bar{V}_- = 0$. This yields the Clarke–transformed voltage for balanced power systems in the form

$$s_k = \bar{V}_+ e^{j\omega k}. \quad (31)$$

and a correct reading of the nominal system frequency. On the other hand, the unbalanced phase voltage conditions give rise to the negative sequence, \bar{V}_- , which results in a bias in the estimation of the nominal system frequency, as the corresponding term $e^{-j\omega k}$ in (29) rotates in the opposite direction of the true phasor, designated by $e^{j\omega k}$.

Complex Noncircularity as a Signature of Unbalanced Power Systems. Figure 6 shows the scatter plot trajectories of the Clarke voltage in a balanced and two unbalanced system conditions. For a **balanced power system**, the scatter plot of s_k in (31) describes a circle, that is, it has **only one degree of freedom**. In statistical terms, such random process is called second–order circular (or proper) as it exhibits a rotation–independent distribution¹.

Recall from (29) that general **dynamically unbalanced systems** are characterised by $\bar{V}_-^* \neq 0$, that is, by **two degrees of freedom** as exemplified by the the two ellipses in Figure 6 which represent the trajectories for Type C and Type D voltage sags, well known power voltage imbalances further illustrated in the phasor diagram in Figure 8. In statistical terms, this is reflected in s_k assuming a rotation–dependent “non–circular” trajectory on the real–imaginary scatter diagram. This link with noncircular complex statistics forms the basis for simultaneous frequency estimation and fault detection in 3–phase unbalanced power systems [5, 10, 25–30], a key issue in modern low inertia power grids.

Remark 12. Unbalanced system conditions introduce non–circular complex distributions which are characterised by two degrees freedom, a scenario for which conventional complex-valued linear estimation theory with only one available degree of freedom provides suboptimal solutions. Indeed, it was recently shown that the standard strictly linear model when applied to the modelling of unbalanced systems in (27) is inadequate, and a widely linear model is required [5, 31]. The notions of non–circularity and widely linear modelling underpin the proposed adaptive Clarke and Park transforms, explored in the next section.

¹The circularity diagram is a scatter plot of the real part versus the imaginary part of a complex variable. The strict definition of complex (non)circularity involves rotational invariance of the probability density function of a complex-valued random variable and is out of the scope of this article. For more detail, we refer the reader to [23, 24].

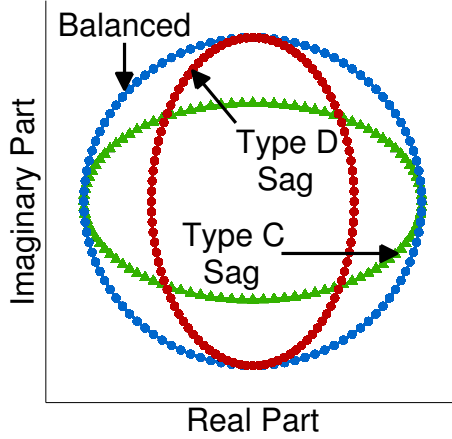


Figure 6: Scatter plot trajectories of the Clarke voltage $v_k = v_\alpha(k) + jv_\beta(k)$. For a balanced system in (1), which is characterised by the nominal frequency $\omega = \omega_\circ$, equal amplitudes of phase voltages $V_a = V_b = V_c$, and equal phases $\phi_a = \phi_b = \phi_c$, the trajectory of Clarke’s voltage v_k is circular (blue line). For unbalanced systems (in this case due to voltage sags), the Clarke voltage trajectories are noncircular (red and green ellipses). See Figure 8 for more detail on voltage sags.

Park Transform as an FM Demodulation Scheme. Similar to the complex-valued representation of the Clarke Transform in (27), the complex-valued version of the Park transform in (12) is given by

$$v_k \stackrel{\text{def}}{=} v_{d,k} + jv_{q,k} \quad (32)$$

which, in analogy to (28) can also be compactly represented as

$$v_k = e^{-j\omega_\circ k} \mathbf{c}^H \mathbf{s}_k = e^{-j\omega_\circ k} s_k, \quad (33)$$

where $s_k = v_{\alpha,k} + jv_{\beta,k}$ is the Clarke voltage. Observe the “circular”, time-varying, rotation frame designated by $e^{-j\omega_\circ k}$ which connects the Clarke and Park transforms.

Remark 13. *From a modern perspective viewpoint, the Park transform in (33) can be interpreted as a frequency demodulation (FM) scheme [32] of the $\alpha\beta$ voltage, whereby the demodulating frequency is the nominal system frequency ω_\circ , as illustrated in Figure 7. The demodulated instantaneous frequency is then obtained from the rate of change of the phase angles of the low-pass filtered signal u_k .*

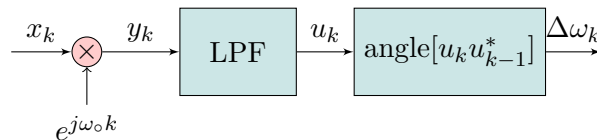


Figure 7: Block diagram of a general fixed frequency demodulation scheme.

Therefore, for a balanced three-phase power system operating at the fundamental frequency ω_\circ , the Park transform yields the stationary positive sequence phasor, shown in Figure 1 and given by

$$v_k = \bar{V}_+. \quad (34)$$

Sources of bias in Park transform when used in dynamically unbalanced Smart Grid. In both current grids which incorporate renewables, and especially in the future Smart Grid, the three-phase voltages will be rarely perfectly balanced and the system frequency will never be at exactly

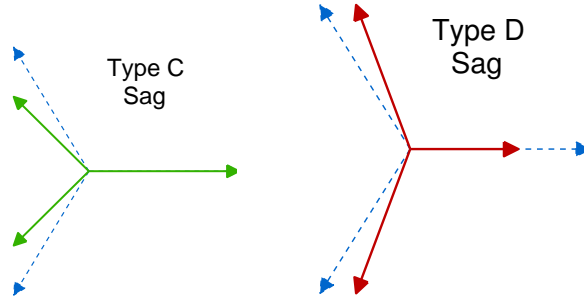


Figure 8: Phasor diagrams of the effects of voltage sags. The dashed blue lines designate a set of balanced three-phase voltage phasors under nominal power system conditions, as in Figure 1. Notice the change in magnitudes and phase separations during faults (Voltage sag C and Voltage sag D in this case).

Table 1: Signal processing interpretations of three-phase transformations.

Transform	Interpretation
Symmetrical [21]	Spatial DFT
Clarke [34]	PCA
Park [19]	FM demodulation

the fundamental frequency [33]. From (29), the complex-valued dq voltage for a general unbalanced three-phase system, which operates at an **off-nominal** system frequency ω , is given by

$$v_k = \bar{V}_+ e^{j(\omega - \omega_o)k} + \bar{V}_-^* e^{-j(\omega + \omega_o)k}. \quad (35)$$

while the Park transform is designed for the nominal frequency, ω_o . Therefore, the imperfect “demodulation” effect of the Park transform at an off-nominal frequency $\omega_o \neq \omega_o$ explains the spurious frequency estimation by the standard Park transform, as illustrated in Figure 10.

On the other hand, if an unbalanced system is operating at the **nominal system frequency**, $\omega = \omega_o$, but **off-nominal phase voltage/phase values**, the Park dq voltage in (35) becomes

$$v_k = \bar{V}_+ + \bar{V}_-^* e^{-j2\omega_o k}. \quad (36)$$

which again is consistent with the output of an FM demodulator. This paves the way for the treatment of power system imbalances from the Communication Theory perspective, as summarised in Table 1.

Remark 14. *Figure 9 shows that during unbalanced system conditions, the optimal reference frames (basis vectors) for the $\alpha\beta$ and dq voltages are different from the nominal ones defined by the classical Park and Clarke transforms.*

Table 2 summarises the functional expressions for the Clarke and Park transforms under both balanced and unbalanced conditions of the electricity grid. As the Clarke and Park transforms will not yield accurate outputs under unbalanced system conditions (noncircular), their adaptive versions are required to enable: i) accounting for voltage imbalances to provide a dynamically balanced Clarke output (circular), and ii) tracking instantaneous changes in system frequency through an “adaptive” Park transform.

Teaching Old Power Systems New Tricks: Adaptive Clark & Park Transforms

It has been widely accepted that the minimum mean square error (MMSE) estimator for a complex-valued process, y_k , based on a complex-valued regressor, \mathbf{x}_k is a straightforward extension of the

	Power System Condition	
Transform	Balanced	Unbalanced
Clarke [34]	$\bar{V}_+ e^{j\omega k}$	$\bar{V}_+ e^{j\omega k} + \bar{V}_- e^{-j\omega k}$
Park [19]	\bar{V}_+	$\bar{V}_+ e^{j(\omega-\omega_0)k} + \bar{V}_-^* e^{-j(\omega+\omega_0)k}$

Table 2: Output of the Clarke and Park transformations.

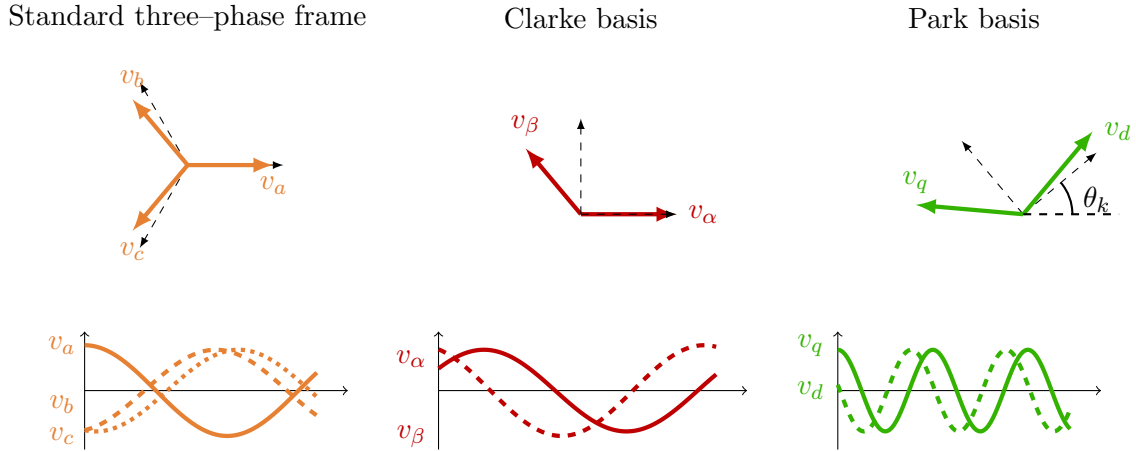


Figure 9: Effects of unbalanced three-phase power systems on the accuracy of classical three-phase reference frames for their analysis. Observe that both standard Clarke and Park reference frames are unsuitable for unbalanced phase voltages/phases and the operation at off-nominal frequencies, as exemplified by the oscillatory Park output for a static off-nominal frequency, instead of the two straight lines, as in Figure 1.

corresponding real-valued one, and assumes the **strictly linear** form

$$\hat{y}_k = E\{y_k | \mathbf{x}_k\} = \mathbf{h}^H \mathbf{x}_k \quad (37)$$

where \mathbf{h} is a set of complex-valued coefficients. However, given that

$$\hat{y}_{r,k} = E\{y_{r,k} | \mathbf{x}_{r,k}, \mathbf{x}_{i,k}\} \quad \hat{y}_{i,k} = E\{y_{i,k} | \mathbf{x}_{r,k}, \mathbf{x}_{i,k}\} \quad (38)$$

and using the well known identities, $x_r = (x + x^*)/2$ and $x_i = (x - x^*)/2j$, the correct estimator for the generality of complex data is **widely linear**, and is given by [23, 35]

$$\hat{y}_k = \mathbf{h}^H \mathbf{x}_k + \mathbf{g}^H \mathbf{x}_k^H \quad (39)$$

A comparison with unbalanced power systems shows that the general unbalanced $\alpha\beta$ voltage in (29), which is a sum of two complex-valued sinusoids rotating in opposite directions, can be represented by a widely linear autoregressive (WLAR) model, given by [5, 23, 35]

$$s_k = h^* s_{k-1} + g^* s_{k-1}^*, \quad (40)$$

Remark 15. A comparison with (29) and (35) shows that the WLAR coefficients $h, g \in \mathbb{C}$ contain the information related to the system frequency, ω , together with providing the desired additional degree of freedom – a pre-requisite for the analysis of unbalanced power system.

The level of voltage imbalance in the power system can be defined through the voltage unbalance factor (VUF), given by [33]

$$\text{VUF} : \quad \kappa \stackrel{\text{def}}{=} \bar{V}_- / \bar{V}_+. \quad (41)$$

so that, as showed in [5], the system frequency can be expressed through the WLAR coefficients, h and g , and the VUF, κ , to yield

$$e^{j\omega} = h^* + g^* \kappa \quad \text{and} \quad e^{-j\omega} = h^* + \frac{g^*}{\kappa^*}. \quad (42)$$

It is snow straightforward to solve for the system frequency, ω , and VUF as

$$e^{j\omega} = \text{Re}\{h\} + j\sqrt{\text{Im}^2\{h\} - |g|^2}, \quad (43)$$

$$\kappa = \frac{\bar{V}_-}{\bar{V}_+} = \frac{j}{g^*} \left(\text{Im}\{h\} + \sqrt{\text{Im}^2\{h\} - |g|^2} \right). \quad (44)$$

Self-Balancing Clarke and Park Transforms

The knowledge of the VUF, κ in (44), proves instrumental in eliminating the negative sequence phasor, \bar{V}_- , from the $\alpha\beta$ voltage s_k . To this end, consider the expression [36]

$$m_k \stackrel{\text{def}}{=} \sqrt{2} (s_k - \kappa^* s_k^*) \quad (45)$$

$$\begin{aligned} &= \bar{V}_+ e^{j\omega k} + \bar{V}_-^* e^{-j\omega k} - \frac{\bar{V}_-^*}{\bar{V}_+^*} \left(\bar{V}_+^* e^{-j\omega k} + \bar{V}_- e^{j\omega k} \right) \\ &= \bar{V}_+ (1 - |\kappa|^2) e^{j\omega k}. \end{aligned} \quad (46)$$

whereby the value of κ is readily available from the WLAR coefficients in (44). This makes it possible to eliminate the effects of voltage imbalance on the Clarke's $\alpha\beta$ voltage in the form

$$\bar{m}_k = m_k / (1 - |\kappa|^2) = \bar{V}_+ e^{j\omega k}. \quad (47)$$

Remark 16. *The voltage \bar{m}_k contains only the positive voltage sequence \bar{V}_+ and is immune to the effects of system imbalance, reflected through the non-zero negative sequence \bar{V}_- . The operation in (47) can be regarded as an adaptive Clarke transform, the output of which is always identical to the correct $\alpha\beta$ voltage for a balanced system.*

Finally, from the estimated time-varying values of the drifting system frequency (through $e^{j\omega k}$ in (43) and κ_k in (44)), the adaptive Clarke and Park transforms can be summarised as [15]

$$\text{Adaptive Clarke transform : } \bar{m}_k = \sqrt{2}(s_k - \kappa_k^* s_k^*) / (1 - |\kappa_k|^2) \quad (48a)$$

$$\text{Adaptive Park transform : } \tilde{m}_k = e^{-j\omega_k k} \bar{m}_k, \quad (48b)$$

where \bar{m}_k is the adaptive $\alpha\beta$ (Clarke) voltage while \tilde{m}_k is the adaptive dq (Park) voltage.

For real-time adaptive operation, the adaptive Clarke and Park transforms can be implemented based on (48a)–(48b), and using a suitable adaptive learning algorithm (e.g. least mean square (LMS) or Kalman filter) to track the VUF, κ_k , and system frequency, ω_k . For illustration, we present the adaptive Clarke/Park transform in Algorithm 1, with the augmented complex least mean square (ACLMS) [23, 37] used to estimate the information bearing WLAR coefficients h and g .

Remark 17. *The adaptive “balancing” versions of the Clarke and Park transforms perform accurately the respective dimensionality reduction and rotation operations, regardless of the drifts in system frequency or level of voltage/phase imbalance. Table 3 summarises the functional expressions for these adaptive transforms, which make it possible to use standard analysis techniques designed for nominal conditions in general unbalanced systems, resulting in a bias-free operation.*

Figure 10 shows the direct and quadrature Park voltages, $v_{d,k}$ and $v_{q,k}$, obtained from both the original Park transform defined in (12), and the adaptive Park transform, \tilde{m}_k in (48b) and Algorithm 1. Observe the oscillating output of the original Park transform (broken red line) when the system frequency suddenly changed to a lower, off-nominal, value starting from $t = 2s$. On the other hand, the adaptive Park transform was able to converge to a stationary (non-oscillatory) correct phasor soon after this system imbalance. Figure 11 further supports the “balancing” nature of the Adaptive Clarke transform through the corresponding circularity diagrams of v_α on the x -axis versus v_β on the y -axis. The circular profile for the adaptive $\alpha\beta$ voltage, \bar{m}_k in (48a), in the presence of Type D voltage sag indicates its successful operation.

Transform	Power System Condition	
	Balanced	Unbalanced
Clarke [34]	$\bar{V}_+ e^{j\omega k}$	$\bar{V}_+ e^{j\omega k} + \bar{V}_- e^{-j\omega k}$
Balancing [36]	$\bar{V}_+ e^{j\omega k}$	$(1 - \kappa ^2) \bar{V}_+ e^{j\omega k}$
<i>Adaptive Clarke</i>	$\bar{V}_+ e^{j\omega k}$	$\bar{V}_+ e^{j\omega k}$
Park [19]	\bar{V}_+	$\bar{V}_+ e^{j(\omega - \omega_0)k} + \bar{V}_-^* e^{-j(\omega + \omega_0)k}$
<i>Adaptive Park</i>	\bar{V}_+	\bar{V}_+

Table 3: Comparison of the classical static three-phase transforms.

Algorithm 1. Adaptive Clarke/Park Transform

Input: Original three-phase voltages, s_k , learning rate, μ

At each time instant $k > 0$:

- 1: Obtain the Clarke transform : $s_k = \sqrt{2} \mathbf{c}^H \mathbf{s}_k$
- 2: Update the weights of ACLMS

$$\begin{aligned} \varepsilon_k &= s_k - (h_{k-1}^* s_{k-1} + g_{k-1}^* s_{k-1}^*) \\ h_k &= h_{k-1} + \mu s_{k-1} \varepsilon_k^* \\ g_k &= g_{k-1} + \mu s_{k-1}^* \varepsilon_k^* \end{aligned}$$

- 3: Use (48a) and (48b) to obtain κ_k and $e^{j\omega k}$
 - 4: Calculate adaptive Clarke transform: $\bar{m}_k = (s_k - \kappa_k^* s_k^*) / (1 - |\kappa_k|^2)$
 - 5: Calculate adaptive Park transform: $\bar{m}_k = e^{-j\omega_k k} \bar{m}_k$
-

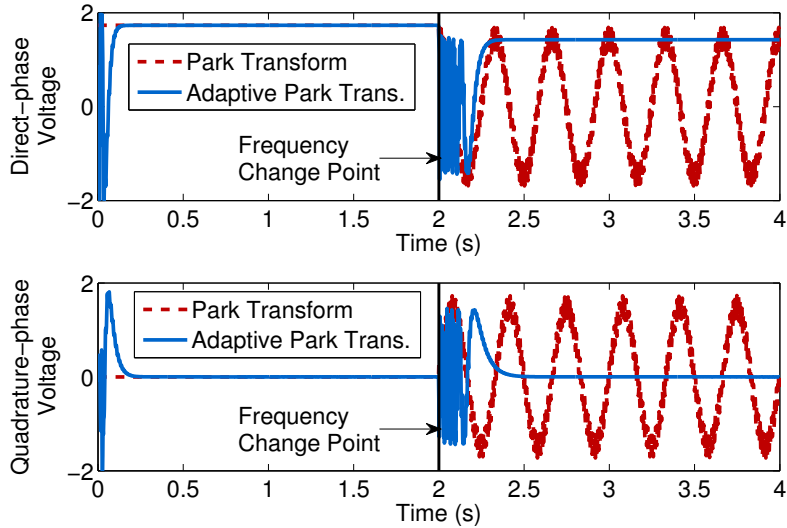


Figure 10: Operation of the classical and adaptive Park Transforms in frequency estimation in unbalanced power grids. Observe the self-stabilising nature of the adaptive Park transform in the presence of system imbalance (frequency drop) starting from $t = 2s$.

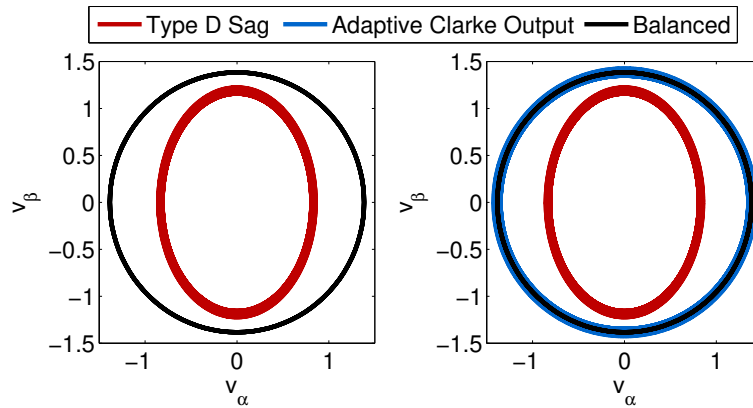


Figure 11: Self-balancing nature of the adaptive Clarke transform at a nominal system frequency, ω_o , but in the presence of Type D voltage sag, indicated by the red ellipse. The adaptive Clarke transform yields a circular (balanced) $\alpha\beta$ voltage, \bar{m}_k in (48a) (blue circle), which coincides with the optimal “balanced” conditions (black circle).

Conclusion

The operation of the future and almost permanently dynamically unbalanced Smart Grids requires close cooperation and convergence between the Power Systems and Data Analytics communities, such as those working in Signal Processing and Machine Learning. A major prohibitive factor in this endeavour has been a lack of common language; for example, the most fundamental techniques, such the Clarke and Park transform introduced respectively in 1943 and 1929, have been designed from a Circuit Theory perspective and only for balanced “nominal” system conditions, characterised by high grid inertia. This renders such methodologies both inadequate for the demands of modern, dynamically unbalanced, Smart Grids and awkward for linking up with Data Analytics communities. To help bridge this gap, we have provided modern interpretations of the the Clarke and related transforms through the modern subspace, demodulation, and complex non-circularity concepts. These have served as a mathematical lens into the inadequacies of current methodologies under unbalanced power system conditions, and have enabled us to create a framework for the understanding and mitigation of the effects of off-nominal system frequency and dynamically unbalanced phase voltages and phases. All in all, such a conceptual insight permits seamless migration of ideas, in a bidirectional way, between these normally disparate communities and helps demystify power system analysis for Data Analytics practitioners.

It is fitting to conclude the article with a quote from J.E. Brittain’s article on Edith Clarke [1], which states

She [Clarke] translated what many engineers found to be esoteric mathematical methods into graphs or simpler forms during a time when power systems were becoming more complex and when the initial efforts were being made to develop electromechanical aids to problem solving.

It is our hope that this modern perspective of the Clarke and related transforms will help extend the legacy of Edith Clarke well into the Information Age, in addition to empowering analysts with enhanced intuition and freedom in algorithmic design. It further opens up new possibilities in the otherwise prohibitive applications of Clarke-inspired transforms in future low inertia Smart Grids.

References

- [1] J. E. Brittain, “From Computer to Electrical Engineer: The Remarkable Career of Edith Clarke,” *IEEE Transactions on Education*, vol. 28, pp. 184–189, Nov 1985.
- [2] E. Clarke, “Calculator,” US Patent 1552113, September 1925.

- [3] M. Canteli, A. Fernandez, L. Eguiluz, and C. Estebanez, “Three-phase adaptive frequency measurement based on Clarke’s transformation,” *IEEE Transactions on Power Delivery*, vol. 21, no. 3, pp. 1101–1105, 2006.
- [4] D. Barbosa, U. C. Netto, D. V. Coury, and M. Oleskovicz, “Power transformer differential protection based on clarke’s transform and fuzzy systems,” *IEEE Transactions on Power Delivery*, vol. 26, pp. 1212–1220, April 2011.
- [5] Y. Xia, S. Douglas, and D. Mandic, “Adaptive frequency estimation in smart grid applications: Exploiting noncircularity and widely linear adaptive estimators,” *IEEE Signal Processing Magazine*, vol. 29, no. 5, pp. 44–54, 2012.
- [6] G. W. Arnold, “Challenges and opportunities in smart grid: A position article,” *Proceedings of the IEEE*, vol. 99, no. 6, pp. 922–927, 2011.
- [7] M. H. J. Bollen, “Voltage sags in three-phase systems,” *IEEE Power Engineering Review*, vol. 21, no. 9, pp. 8–15, 2001.
- [8] D. Nakafuji, “Personal communication,” heco, hi, usa, 2011.
- [9] M. H. J. Bollen, I. Y. H. Gu, S. Santoso, M. F. McGranaghan, P. A. Crossley, M. V. Ribeiro, and P. F. Ribeiro, “Bridging the gap between signal and power,” *IEEE Signal Processing Magazine*, vol. 26, no. 4, pp. 11–31, 2009.
- [10] D. P. Mandic, Y. Xia, and D. Dini, “Frequency estimation,” US Patent 9995774, June 2018.
- [11] T. Routtenberg and Y. C. Eldar, “Centralized identification of imbalances in power networks with synchrophasor data,” *IEEE Transactions on Power Systems*, vol. 33, pp. 1981–1992, March 2018.
- [12] T. Routtenberg and L. Tong, “Joint frequency and phasor estimation under the KCL constraint,” *IEEE Signal Processing Letters*, vol. 20, pp. 575–578, June 2013.
- [13] A. Pradhan, A. Routray, and A. Basak, “Power system frequency estimation using least mean square technique,” *IEEE Transactions on Power Delivery*, vol. 20, no. 3, pp. 1812–1816, 2005.
- [14] A. Routray, A. K. Pradhan, and K. P. Rao, “A novel Kalman filter for frequency estimation of distorted signals in power systems,” *IEEE Transactions on Instrumentation and Measurement*, vol. 51, pp. 469–479, Jun 2002.
- [15] S. Kanna and D. P. Mandic, “Self-stabilising adaptive three-phase transforms via widely linear modelling,” *Electronics Letters*, vol. 53, no. 13, pp. 875–877, 2017.
- [16] Y. F. Huang, S. Werner, J. Huang, N. Kashyap, and V. Gupta, “State estimation in electric power grids: Meeting new challenges presented by the requirements of the future grid,” *IEEE Signal Processing Magazine*, vol. 29, pp. 33–43, Sept 2012.
- [17] “Park, Inverse Park and Clarke, Inverse Clarke Transformation: MSS Software Implementation,” Tech. Rep. 50200359-0/11.13, Microsemi Corporation, Aliso Viejo, California, January 2013.
- [18] S. M. Kay, *Fundamentals of Statistical Signal Processing: Estimation Theory*. Prentice Hall International, Inc, 1993.
- [19] R. H. Park, “Two-reaction theory of synchronous machines generalized method of analysis – Part I,” *Transactions of the American Institute of Electrical Engineers*, vol. 48, pp. 716–727, July 1929.
- [20] J. Shlens, “A tutorial on principal component analysis,” *CoRR*, vol. abs/1404.1100, 2014.

- [21] C. L. Fortescue, "Method of symmetrical co-ordinates applied to the solution of polyphase networks," *Transactions of the American Institute of Electrical Engineers*, vol. 37, no. 2, pp. 1027–1140, 1918.
- [22] G. C. Paap, "Symmetrical components in the time domain and their application to power network calculations," *IEEE Transactions on Power Systems*, vol. 15, pp. 522–528, May 2000.
- [23] D. P. Mandic and V. S. L. Goh, *Complex valued nonlinear adaptive filters: Noncircularity, widely linear and neural models*. Wiley, 2009.
- [24] P. J. Schreier and L. L. Scharf, *Statistical signal processing of complex-valued data: The theory of improper and noncircular signals*. Cambridge University Press, 2010.
- [25] L. Zhang and M. H. J. Bollen, "Characterisation of voltage dips in power systems," *IEEE Transactions on Power Delivery*, vol. 15, no. 2, pp. 827–832, 2000.
- [26] M. Bollen, "Characterisation of voltage sags experienced by three-phase adjustable-speed drives," *IEEE Transactions on Power Delivery*, vol. 12, no. 4, pp. 1666–1671, 1997.
- [27] M. Bollen and L. Zhang, "Different methods for classification of three-phase unbalanced voltage dips due to faults," *Electric Power Systems Research*, vol. 66, no. 1, pp. 59 – 69, 2003.
- [28] S. Kanna, D. H. Dini, Y. Xia, S. Y. Hui, and D. P. Mandic, "Distributed widely linear Kalman filtering for frequency estimation in power networks," *IEEE Transactions on Signal and Information Processing over Networks*, vol. 1, pp. 45–57, March 2015.
- [29] Y. Xia, Z. Blazic, and D. Mandic, "Complex-valued least squares frequency estimation for unbalanced power systems," *IEEE Transactions on Instrumentation and Measurement*, vol. PP, no. 99, pp. 1–1, 2014.
- [30] Y. Xia and D. Mandic, "Augmented MVDR spectrum-based frequency estimation for unbalanced power systems," *IEEE Transactions on Instrumentation and Measurement*, vol. 62, no. 7, pp. 1917–1926, 2013.
- [31] B. Picinbono and P. Chevalier, "Widely linear estimation with complex data," *IEEE Trans. Signal Process.*, vol. 43, no. 8, pp. 2030–2033, 1995.
- [32] M. Akke, "Frequency estimation by demodulation of two complex signals," *IEEE Transactions on Power Delivery*, vol. 12, pp. 157–163, Jan 1997.
- [33] A. von Jouanne and B. Banerjee, "Assessment of voltage unbalance," *IEEE Trans. Power Del.*, vol. 16, pp. 782–790, Oct 2001.
- [34] E. Clarke, *Circuit Analysis of A.C. Power Systems*. New York: Wiley, 1943.
- [35] B. Picinbono, "On Circularity," *IEEE Transactions on Signal Processing*, vol. 42, no. 12, pp. 3473–3482, 1994.
- [36] Y. Xia, K. Wang, W. Pei, and D. P. Mandic, "A balancing voltage transformation for robust frequency estimation in unbalanced power systems," in *Proc. of the Asia Pacific Signal and Information Processing Association Annual Summit and Conference (APSIPA)*, pp. 1–6, Dec 2014.
- [37] S. Javidi, M. Pedzisz, S. L. Goh, and D. P. Mandic, "The augmented complex least mean square algorithm with application to adaptive prediction problems," *Proc. 1st IARP Workshop on Cognitive Information Processing*, pp. 54–57, 2008.